Computed Tomographic X-ray Velocimetry

S. Dubsky,[1,2] R.A. Jamison,[1,2] S.C. Irvine,[3] K.K.W. Siu,[3,4] K. Hourigan,[1,2] and A.Fouras[1,2a]

[1] *Division of Biological Engineering, Monash University, Melbourne 3800, Australia*
[2] *Department of Mechanical & Aerospace Engineering, FLAIR, Monash University, Melbourne 3800, Australia*
[3] *School of Physics, Monash University, Melbourne 3800, Australia*
[4] *Monash Centre for Synchrotron Science, Monash University, Melbourne 3800, Australia*

Abstract. An X-ray velocimetry technique is described which provides three components of velocity measurement in three-dimensional space. Current X-ray velocimetry techniques, which use particle images taken at a single projection angle, are limited to two components of velocity measurement, and are unable to measure in three dimensions without a priori knowledge of the flow field. The proposed method uses multiple projection angles to overcome these limitations. The technique uses a least-squares iterative scheme to tomographically reconstruct the three-dimensional velocity field directly from two-dimensional image pair cross-correlations, without the need to reconstruct three-dimensional particle images. Synchrotron experiments demonstrate the effectiveness of the technique for blood flow measurement in opaque vessels, with applications for the diagnosis and treatment of cardiovascular disease.

Keywords: blood flow measurement; tomography; least squares approximations; synchrotrons; velocity measurement.
PACS: 87.57.qp

INTRODUCTION

The ability to measure three-dimensional (3D) blood flow fields *in vivo* is an important capability for studying the effects of blood flow properties on the development, diagnosis and treatment of cardiovascular diseases, such as atherosclerosis [1,2]. To gain useful information from *in vivo* blood flow field measurements, non-invasive measurement through opaque tissue at high resolution is required.

Currently available techniques for flow field measurement in opaque vessels, such as magnetic resonance imaging based techniques [3,4], suffer from poor spatial and temporal resolution, limiting the application of these techniques for *in vivo* analysis.

Particle-image velocimetry (PIV) is an established flow measurement technique, in which the displacement of tracer particles is determined using cross-correlation of regions within particle image pairs [5,6]. Several variants exist for volumetric flow analysis [7-9], which require reconstruction of the particle image in 3D space, followed by either 3D particle tracking or 3D cross-correlation within this volume. This requires each tracer particle to be discernable from all imaging angles, limiting the maximum particle seeding density, thus reducing spatial resolution. Also, PIV techniques are typically applied using visible light, necessitating an optically transparent sample.

X-rays allow high resolution imaging through opaque tissue, making this imaging mode ideal for *in vivo* measurement. X-ray phase contrast imaging exploits the high coherence of third-generation synchrotron radiation, whilst the high flux from these sources permits rapid imaging. A large propagation distance between the sample and the detector allows the incident X-ray waves, which are slightly refracted at surface interfaces, to interfere at the detector plane, generating intensity fringes which result in edge enhancement. In this way, propagation-based X-ray phase-contrast imaging (PCI) provides the ability to differentiate soft tissue, and even red blood cells, a capability not available through typical absorption based X-ray imaging [10-12].

Several recent studies have combined PCI with PIV to yield planar [13,14] or volumetric flow measurements [11,15,16]. X-ray PIV has also been performed using absorption contrast imaging with medical X-ray sources [17]. The X-ray PIV techniques described in these studies use particle images taken at

[a] Corresponding author: fouras@eng.monash.edu.au

CP1266, *6th International Conference on Medical Applications of Synchrotron Radiation,* edited by K. K. W. Siu

a single viewing angle, which contain no particle displacement information in the direction parallel to the X-ray beam, limiting X-ray PIV to two component velocity measurements. Also, no information regarding the velocity profile in the dimension perpendicular to the image plane is available, and therefore 3D measurements are not possible without prior knowledge of the flow. The use of multiple projection angles to overcome this limitation has been suggested [12,16,18], however no implementation of this concept has appeared in the literature. We have developed an X-ray PIV technique that uses data obtained from multiple viewing angles for tomographic reconstruction of the 3D flow-field [19]. The technique, computed tomographic X-ray velocimetry (CTXV), combines phase-contrast X-ray imaging with PIV and computed tomography (CT).

Computed tomography is a technique used to reconstruct an object in 3D space from two-dimensional projections. Typically, integrated object density in the projection direction is calculated from the X-ray attenuation, which will be proportional to the pixel intensity values on a digital projection image. The object is then reconstructed from projection images taken at different viewing angles, back-projection or algebraic methods [20]. Variants also exist for reconstruction of objects from few projection angles, which use iterative reconstruction methods, often exploiting prior knowledge of the sample, for example that it is made up of a single material [21,22].

We have previously demonstrated that the cross-correlation functions calculated from X-ray particle image pairs represent a probability density function (PDF) of the velocity within the projected volume [15,23]. In CTXV, information regarding the three-components of velocity in 3D space is obtained by imaging from multiple projection angles, and this is then used to tomographically reconstruct the velocity field directly, without the need to reconstruct a volumetric particle image.

EXPERIMENTAL PROCEDURE

Experiments were conducted at the SPring-8 Synchrotron, Hyogo, Japan, using the high-resolution medical imaging beam-line (BL20XU). The source to sample distance of 245 m provides highly coherent X-rays for phase contrast imaging. A Si-111 double crystal monochromator was used to provide a monochromatic beam energy of 25 keV.

Sample

The sample used was an optically opaque plastic arterial model, with an average diameter of 950 μm. manufactured using Objet™ 3D-printing technology. The geometry was chosen to mimic a stenosed artery, generating a 3D flow field similar to that which would occur *in vivo*. Blood was pumped through the model at a flow-rate of 4.8 μl/mn, using a syringe pump (WPI Inc. UMP2). While PCI has been successful in imaging red blood cells as tracer particles [11,14], to increase signal to noise ratio, the blood was seeded with gas micro-bubbles. As PCI creates high contrast at a gas-liquid interface, microbubbles represent an ideal flow tracing media for this imaging modality. The ultrasound contrast agent Definity® (Bristol-Myers Squibb Medical Imaging Inc.) was used. When activated, Definity® forms a stable, injectable, homogeneous suspension of perfluorocarbon-filled microbubbles, with a mean diameter of 2.5 μm [24].

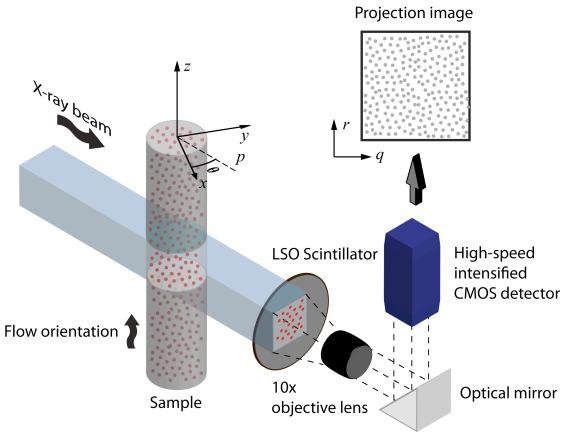

FIGURE 1. (Color) Schematic diagram of experimental imaging setup. Cartesian co-ordinates *x,y,z* are fixed to the sample, and rotated at an angle θ from the beam axis *p*.

Imaging Setup

The imaging setup is shown in Figure 1. X-rays project through the sample onto a scintillator, which converts X-ray radiation into visible light. The scintillator is imaged using a high-speed intensified CMOS detector (IDT Inc. X5i, 4 megapixel) through a microscope objective lens, resulting in a magnification of approximately 15× or an effective pixel size of 0.52 μm. An optical mirror removes the detector from the X-ray beam path. A total scan time of less than 10 seconds was achieved through the use of a high-speed intensified camera, which allowed exposure times of 4.5 ms, and a frame rate of 200 Hz. The sample was rotated through 9 projection angles, spaced over 180º, with 195 images taken at each angle. The sample to detector distance was optimized experimentally for phase contrast of the blood-Definity® mixture, and an optimum of 900 mm was found to provide the best signal.

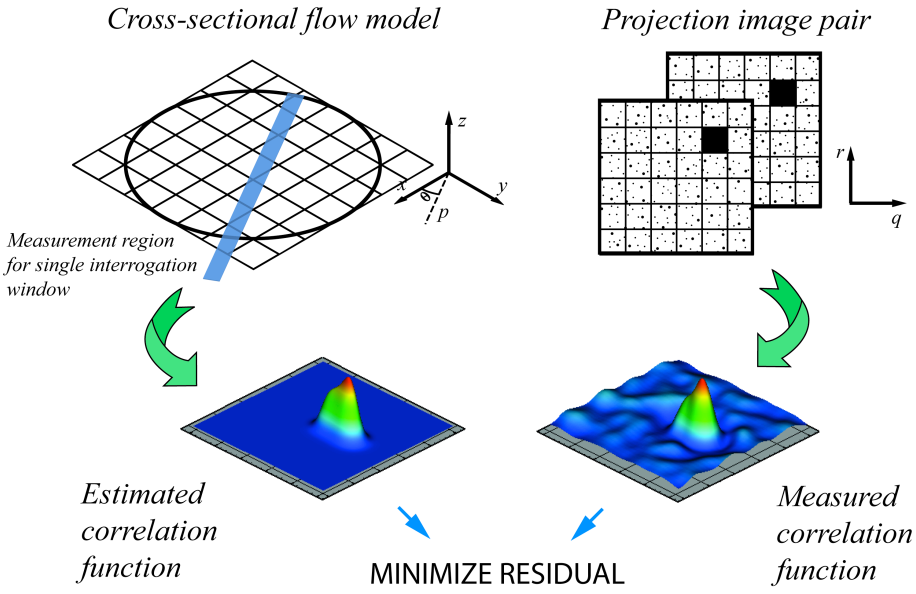

FIGURE 2. (Color) CTXV reconstruction. The residual between estimated and measured cross-correlations is minimized over all interrogation windows and all projection angles simultaneously to yield a cross-sectional flow model which accurately represents the flow field.

Image Preprocessing

X-ray phase-contrast particle images require pre-processing prior to cross-correlation analysis. A spatial high-pass filter was applied to remove the effects of inhomogeneous illumination. Stationary structures such as the vessel walls, monochromator effects, and dust on the detector or associated optics, are removed by average image subtraction. A single-image phase-retrieval algorithm [25] is then implemented to remove phase contrast fringes and improve the images for cross-correlation analysis, as described by Irvine *et al*. [11]

Velocity Reconstruction

Figure 2 outlines the reconstruction method used for CTXV. The particle images are discretised into rectangular interrogation windows and cross-correlation is performed on these windows. For this experiment the interrogation window size was 128×128 pixels with 75% overlap. The volume is reconstructed in axial cross-sections, defined by the rows of the interrogation windows. A rectangular grid model is used to define the cross-sectional flow profile. Velocity components in the x, y and z directions, v_x, v_y, and v_z, are defined at each node in the model. Bi-linear interpolation is used between node points to define the velocity profile in the model space. A point on the model $P(x, y)$ will be projected onto the image plane as $P(q)$, where $q = y\cos(\theta) - x\sin(\theta)$, for a given cross-section in z. Similarly, velocity components are transformed onto the image plane as $v_q = v_y\sin(\theta) - v_x\cos(\theta)$ and $v_r = v_z$, where v_q and v_r are the velocity components in the q and r directions, respectively. Cross-correlation functions are estimated for each interrogation window measurement region by projecting the PDF from the flow model onto the image plane. This projected PDF is convolved with the particle image auto-correlation function to yield the estimated cross-correlation functions. The 3D velocity field reconstruction then becomes a minimization of the error between the cross-correlation functions estimated using the flow model, and those calculated from the X-ray image pairs, for all projection angles. The solution is implemented using the Levenberg-Marquardt algorithm, which performs a non-linear least-squares optimisation. Tikhonov regularization is utilized to improve convergence of the strongly over-specified system, where the regularization function equals the difference between each velocity parameter and the mean of its neighbors, summed over the reconstruction domain.

RESULTS

Figure 3 shows the 3D velocity field of blood flow inside the optically opaque vessel model, measured using CTXV. Maximum velocity reduces as the vessel

geometry expands, as predicted by the conservation of mass. The flow rates determined from the individually reconstructed cross-sections of Figure 3 are all within 2% of that independently measured by the syringe pump setting. The result demonstrates the ability of CTXV to measure all three components of velocity within a volume, with no optical access required.

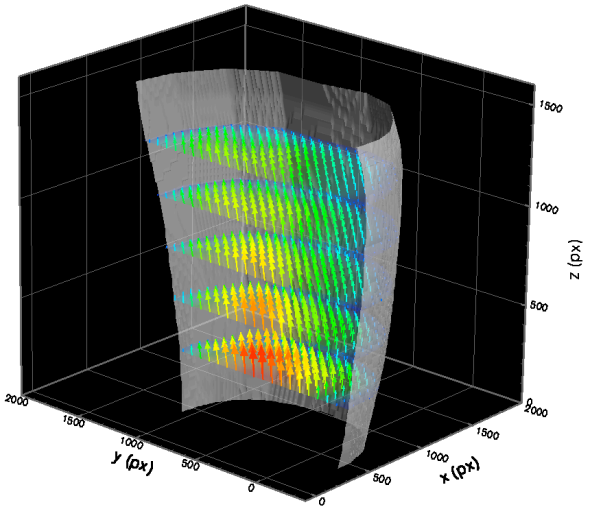

FIGURE 3. (Color) Reconstructed blood velocity field, measured using CTXV. For clarity only half the sample is plotted, with reduced vector resolution in all dimensions. Vector colors represent velocity magnitude.

CONCLUSIONS

The technique presented in this letter represents a significant advancement in X-ray velocimetry, providing the ability to measure 3D blood flow-fields inside opaque vessels. With recent developments in ultra-fast synchrotron imaging [26] and X-ray PIV tracer particles [27], the ability to image flows at physiological rates will allow application of this technique to *in vivo* measurement of blood flow. The short scan time required (less than 10 seconds) and high-resolution measurement makes this technique an ideal tool for research into cardiovascular disease, with future applications for clinical diagnosis and treatment.

ACKNOWLEDGEMENTS

The authors gratefully acknowledge the support of the Japan Synchrotron Radiation Research Institute (JASRI) (under Proposal No. 2008B1969). The authors would like to thank Drs Yoshio Suzuki, Akishi Takeuchi and Kentaro Uesugi (SPring-8/JASRI) for their assistance with the experiments. Support from an Australian Research Council Discovery Grant (DP0877327) is also gratefully acknowledged.

REFERENCES

1. S. Berger and L. Jou, Annu. Rev. Fluid Mech. **32**, 347 (2000).
2. W. Nesbitt, E. Westein, E. Tolouei, J. Fu, J. Carberry, A. Fouras, and S. Jackson, Nat. Med. **15**, 665 (2009).
3. C. Elkins and M. Alley, Exp. Fluids **43**, 823 (2007).
4. D. Bonn, S. Rodts, M. Groenink, S. Rafai, N. Shahidzadeh-Bonn, and P. Coussot, Annu. Rev. Fluid Mech. **40**, 209 (2008).
5. M. Raffel, C. E. Willert, and J. Kompenhans, *Particle Image Velocimetry: A Practical Guide* (Springer, Berlin, Germany, 1998).
6. R. J. Adrian, Exp. Fluids **39**, 159 (2005).
7. G. Elsinga, F. Scarano, B. Wieneke, and B. van Oudheusden, Exp. Fluids **41**, 933 (2006).
8. C. Willert and M. Gharib, Exp. Fluids **12**, 353 (1992).
9. D. Barnhart, R. Adrian, and G. Papen, Appl. Opt. **33**, 7159 (1994).
10. S. Wilkins, T. Gureyev, D. Gao, A. Pogany, and A. Stevenson, Nature (London) **384**, 335 (1996).
11. S. Irvine, D. Paganin, S. Dubsky, R. Lewis, and A. Fouras, Appl. Phys. Lett. **93**, 153901 (2008).
12. A. Fouras, M. Kitchen, S. Dubsky, R. Lewis, S. Hooper, and K. Hourigan, J. Appl. Phys. **105**, 102009 (2009).
13. S. J. Lee and G. B. Kim, J. Appl. Phys. **94**, 3620 (2003).
14. G. B. Kim and S. J. Lee, Exp. Fluids **41**, 195 (2006).
15. A. Fouras, J. Dusting, R. Lewis, and K. Hourigan, J. Appl. Phys. **102**, 064916 (2007).
16. K. Im, K. Fezzaa, Y. Wang, X. Lui, and M. Lai, Appl. Phys. Lett. **90**, 091919 (2007).
17. S. J. Lee, G. B. Kim, D. H. Yim, and S. Y. Jung, Rev. Sci. Instrum. **80**, 033706 (2009).
18. A. Fouras, J. Dusting, J. Sheridan, M. Kawahashi, H. Hirahara, and K. Hourigan, Clin. Exp. Pharmacol. Physiol. **36**, 238 (2009).
19. S. Dubsky, R.A. Jamison, S.C. Irvine, K.K.W. Siu, K. Hourigan, and A. Fouras, Appl. Phys. Lett. **96**, 023702 (2010).
20. A. Kak and M. Slaney, *Principles of Computerized Tomographic Imaging* (IEEE, New York, 1988).
21. S. Soussen and A. Mohammad-Djafari, IEEE Trans. Image Process. **13**, 1507 (2004).
22. G. Myers, D. Paganin, T. Gureyev, and S. Mayo, Opt. Express **16**, 908 (2008).
23. A. Fouras, D. Lo Jacono, C. V. Nguyen, and K. Hourigan, Exp. Fluids **47**, 569 (2009).
24. E. Quaia, *Contrast Media in Ultrasonography* (Springer, Berlin, 2005).
25. D. Paganin, S. Mayo, T. Gureyev, P. Miller, and S. Wilkins, J. Microsc. **206**, 33 (2002).
26. Y. Wang, X. Liu, K. Im, W. Lee, J. Wang, K. Fezzaa, D. Hung, and J. Winkelman, Nat. Phys. **4**, 305 (2008).
27. G. B. Kim, N. Y. Lim, and S. J. Lee, Microfluid. Nanofluid. **6**, 419 (2009).